

# Fast repetition rate fluorometry (FRRF) measuring phytoplankton productivity: A case study at the entrance to the Gulf of Finland, Baltic Sea

Mika P. Raateoja

*Finnish Institute of Marine Research, P.O. Box 33, FIN-00931 Helsinki, Finland (e-mail: mika.raateoja@fimr.fi)*

Raateoja, M. P. 2004: Fast repetition rate fluorometry (FRRF) measuring phytoplankton productivity: A case study at the entrance to the Gulf of Finland, Baltic Sea. *Boreal Env. Res.* 9: 263–276.

The fast repetition rate (FRR) fluorometry, based on variable fluorescence of chlorophyll *a*, has been introduced as a potential tool to evaluate the primary productivity (PP) in aquatic systems. I measured PP *in situ* with both the <sup>14</sup>C and the FRR techniques at the entrance to the Gulf of Finland, Baltic sea, and noticed that the relation between the <sup>14</sup>C-based ( $P_b$ ) and the FRR-based ( $P_f$ ) estimates of PP was non-linear. This discrepancy between  $P_f$  measuring the rate of linear photosynthetic electron flow, and  $P_b$  measuring the rate of C fixation should be resolved before the PP can be reasonably estimated with the FRR technique. The deviation from linearity took place at irradiances above 200  $\mu\text{mol quanta m}^{-2} \text{s}^{-1}$ , since  $P_b$  reached light-saturation at lower irradiances than did  $P_f$ . Within the regression fits, the daily variability in  $P_b$  explained at least 85% of the daily variability in  $P_f$  (a total of four days,  $n = 11$  on each day). The period of time over which PP was determined was substantially different for the two approaches; over 2 h for  $P_b$ , and approximately 10 s for  $P_f$ . Consequently, most of the deviation around the resulting fits was caused by the sensitivity of the FRR technique to the momentary incident irradiance at the time of the measurement. The FRR-based photosynthetic efficiency of phytoplankton in the upper parts of the water column could be divided into three layers: reduced levels in the near-surface layer due to inhibiting effect of supraoptimal irradiance, the layer beneath this having the highest levels, and the deepest layer inhabited by a senescent algal population characterized by lowered levels.

## Introduction

One of the future prospects for aquatic remote sensing is a synoptic determination of the micro-algal productivity over large oceanic regions, which would clarify the role of the oceans in the global carbon cycle. As the conventional primary productivity (PP) techniques cannot be applied as remote sensing tools, various radiometric

techniques have been introduced to fill the void. The one presented here, the fast repetition rate (FRR) technique (Kolber and Falkowski 1992), is based on the variable fluorescence characteristics of the phytoplankton.

The FRR technique has been widely utilized in the *in situ* research on phytoplankton. These studies have concerned (i) the nutritional status of the algae, and their physiological responses to

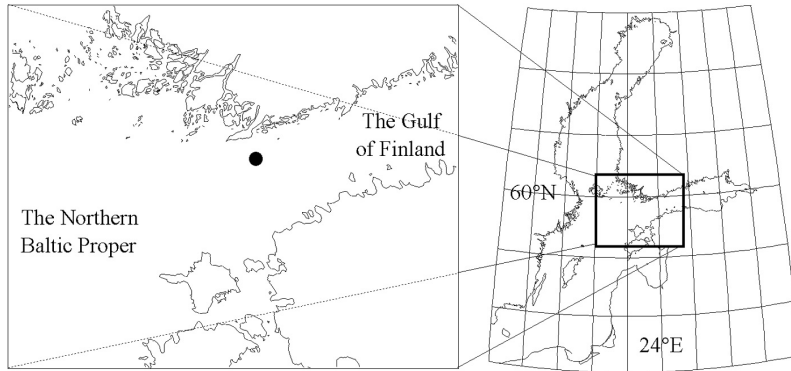


**Fig. 1.** The study area. The location of the sampling site (59°42'N, 23°38'E) is indicated with a black dot.

nutrient limitation (e.g. Sosik and Olson 2002, Hiscock *et al.* 2003), (ii) algal photoinhibition due to excessive visible and/or UV radiation, and photoprotection against them (e.g. Vassiliev *et al.* 1994, Behrenfeld *et al.* 1998), (iii) algal physiological responses to the interaction of changing nutrient and light fields (e.g. Babin *et al.* 1996, Timmermans *et al.* 2001). Recently, Chekalyuk *et al.* (2000) introduced a LIDAR fluorometer based on a pump-and-probe technique (Falkowski *et al.* 1986) that is a predecessor to the FRR technique. This instrument operates from an airborne platform, and is thus able to detect the variable fluorescence characteristics over large sea areas almost synoptically. The authors predict the introduction of an FRR/LIDAR system in the near future. This would be a remote sensing tool of a considerable value, allowing the remote monitoring of the algal photosynthetic characteristics in a highly sensitive manner.

The FRR technique is capable of real-time high-frequency determinations of a suite of the algal photosynthetic parameters, allowing the observation of the algal dynamics with an extended temporal resolution (Falkowski and Kolber 1993, Kolber *et al.* 1998). This is of a particular value whenever the variable fluorescence characteristics of phytoplankton are probed in sea areas where hydrography operates on rather small scales, as compared with the world's oceans. The Baltic Sea is such an oceanic province. The hydrodynamics of the Baltic Sea is complex, showing both spatial and seasonal variability (Voipio 1981). The sea area chosen as the site for this case study, the entrance to the Gulf of Finland, is particularly

distinctive from the hydrodynamic viewpoint (Kononen *et al.* 2003), and shows a pronounced spatiotemporal variability in phytoplankton species composition and biomass (Moisander *et al.* 1997, Kononen *et al.* 1999). Thus, the study area serves as a suitable test site for a technique providing results with high spatiotemporal resolution. The bulk of the PP measurements in the Baltic Sea have been, and still are, carried out using the  $^{14}\text{C}$  technique (Steemann Nielsen 1952). In spite of the fairly long time series of the PP measurements, our knowledge about the PP of this oceanic region is still quite limited, since the  $^{14}\text{C}$  technique cannot provide information on space and time scales that are sufficiently dense.

Here, I used both the  $^{14}\text{C}$  and the FRR techniques to estimate the PP. In order to assess this relation in a natural light environment, I carried out both the  $^{14}\text{C}$  incubations and the FRR-measurements *in situ*. Clarification of this relation serves two purposes. Firstly, alternative methods to the  $^{14}\text{C}$  technique are required for the more robust evaluation of the PP patterns in the dynamic Baltic Sea. Secondly, as long as the relation between the rate of C fixation and the rate of photosynthetic electron flow is not completely resolved, the field  $^{14}\text{C}$  data are of a great value in the validation of the results obtained by the future FRR-based remote sensing systems.

## Material and methods

This study took place at the entrance to the Gulf of Finland in the Baltic Sea between 19 and 30 July 1999 (Fig. 1). The study consisted of two

periods of anchored 48-hour intensive studies, 22–23 July (referred to hereafter as “A”), and 26–27 July (“B”). The four days spent on-station (22, 23, 26, and 27 July) are referred to as “A1”, “A2”, “B1”, and “B2”. Each of the days included three separate casts, starting at 6:00, 8:00 and 10:00 (UTC). Local time was 3 h ahead of UTC time. The sampling depths were 1, 3, 6, and 10 m. The data from the cast at 10:00 on A2 was not acceptable, since the ship shadowed the  $^{14}\text{C}$ -incubations during the cast.

### CTD casts

An SBE 911 Plus CTD system (SeaBird Electronics Ltd.), equipped with a SeaTech chlorophyll fluorometer, probed the water column hourly during the study.

### Radiometric measurements

The downward FRR-based irradiance ( $E_d(\text{FRR})$ , PAR,  $\mu\text{mol quanta m}^{-2} \text{s}^{-1}$ ) at each of the sampling depths was originally measured with a half-spherical collector (Chelsea Instruments Ltd.) connected to the FRR fluorometer. The downward plane irradiance ( $E_d$ , PAR,  $\mu\text{mol quanta m}^{-2} \text{s}^{-1}$ ) at each of the sampling depths was logged twice an hour during the  $^{14}\text{C}$  incubations with a Li-Cor LI-1000 photometer (Li-Cor inc.) equipped with a cosine collector. The average irradiance at each depth during the incubations was calculated by integration over time. The  $E_d(\text{FRR})$  values were subsequently rescaled to the output of the cosine collector. This was done during the seasonal bio-optical monitoring program in the SW coast of Finland, Baltic Sea (91 pairwise comparisons between 0 and 15 m from April to October).

### Nutrients

The concentrations of inorganic nutrients ( $\text{PO}_4^{3-}$  and  $\text{NO}_3^-$ ) from the CTD-rosette samples were determined with a Skalar autoanalyser against national standards SFS 3025 and SFS 3030, respectively, using the spectrophotometric methods described by Grasshoff *et al.* (1999).

### Algal taxonomy and chlorophyll *a*

Biomass of nano- and microphytoplankton species, preserved with acid Lugol's solution, was determined using an inverted microscope (Utermöhl 1958). Biomass is expressed as wet weight (ww,  $\mu\text{g l}^{-1}$ ). The chlorophyll *a* (chl *a*) samples were taken with a Hydrobios sampler. Subsamples of 200 ml were filtered onto Whatman GF/F filters, extracted with 10 ml of 96% ethanol for 24 h, measured fluorometrically with a Perkin-Elmer LS-2B calibrated with a pure chl *a* solution (Sigma), as described in HELCOM (Baltic Marine Environment Protection Commission 1988).

### Fixation of carbon

The apparent net assimilation of C was determined as a  $^{14}\text{C}$ - $\text{CO}_2$  uptake according to Steemann Nielsen (1952) modified by Niemi *et al.* (1983). The activity of the  $^{14}\text{C}$ -labelled  $\text{NaHCO}_3$  aqueous solution ( $^{14}\text{C}$  Agency, Denmark) was  $20 \mu\text{Ci ml}^{-1}$ , and  $4 \mu\text{Ci}$  was added to samples. Three replicate samples were incubated *in situ* in optically transparent Greiner 50-ml tissue culture flasks for 150 to 220 min. The sampling depths were visited in the upward direction in order to have the longest incubation periods for the samples at deeper layers, where the amount of photosynthetically-available radiation, and hence presumably the uptake of labelled carbon, was lower. Radioactivity was measured with a 1219 Rackbeta liquid scintillation counter (LKB Wallac Co, Finland), and the total  $\text{CO}_2$  concentration was calculated with the formula by Buch (1945) and reproduced by Gargas (1975), as described in HELCOM (Baltic Marine Environment Protection Commission 1988). The  $^{14}\text{C}$  incorporation rates were corrected for the dark uptake of  $^{14}\text{C}$ , which was on average 10%, 10%, 17% and 41% of the total uptake at 1, 3, 6, and 10 m, respectively. The  $^{14}\text{C}$ -based biomass-specific *in situ* primary productivity ( $P_b$ , mol C (mol chl *a*) $^{-1} \text{s}^{-1}$ ) was defined as:

$$P_b = P_c \times [\text{chl } a]^{-1} \times 2.068 \times 10^{-2}, \quad (1)$$

where  $P_c$  is the  $^{14}\text{C}$ -based *in situ* primary productivity ( $\text{mg C m}^{-3} \text{h}^{-1}$ ), the unit for chl *a* concentra-

tion is  $\text{mg m}^{-3}$ , and  $2.068 \times 10^{-2}$  is a conversion factor to a molar ratio and a per second rate.

### Variable fluorescence measurements

A fast repetition rate fluorometer (FRRF) FAST<sup>tracka</sup> (Chelsea Instruments Ltd.) was fitted to a protective rack together with the connected external pressure and PAR sensors. The package was lowered into the sea using a stern-mounted A-frame. Calibration of the baseline, scatter, and reference function were carried out according to the manufacturer's instructions. Each FRR observation comprised of five replicates both on the ambient irradiance side and on the dark-adapted side. A replicate was an average of 10 flash sequences. The variable fluorescence parameters  $F_o$ ,  $F_m$ ,  $F$ ,  $F'_m$ ,  $F_v/F_m$ ,  $\Delta F/F'_m$ ,  $\sigma_{\text{PSII}}$ , and  $\sigma'_{\text{PSII}}$  (for the definition of the variable fluorescence parameters, see Appendix) were derived from the raw fluorescence data with the Fasttracka post-processing software FRS v. 1.6 (Chelsea Instruments Ltd.) by an iterative non-linear fitting procedure.

The FRR measurements were carried out after a 10-min dark-adaptation period in order to reach the maximum photochemical efficiency of phytoplankton by ensuring the decay of the fast components of the non-photochemical quenching ( $q_n$ ), and oxidation of the electron transport chain (Krause and Weis 1991, Falkowski 1992). However,  $F'_o$  in the equation of the photochemical quenching ( $q_p$ ) should be measured before the decay of the fast components of  $q_n$  (see Appendix). Calculated this way,  $q_p$  does not strictly reflect the fraction of open photosystem II (PSII) reaction centres. Hence,  $F'_o$  and  $q_p$  were calculated afterwards using equations involving  $F_o$  (Oxborough and Baker 1997).

The calculation of the fluorescence-based *in situ* photosynthetic electron flow  $P_f$  [ $\text{mol e}^- (\text{mol RC})^{-1} \text{s}^{-1}$ ] is based on Falkowski and Kolber (1993) and Falkowski and Raven (1997).

$$P_f = E_d(\text{FRR}) \times \sigma'_{\text{PSII}} \times f' \times q_p \times \phi_{\text{RC}} \times 6.022 \times 10^{-3} \quad (2)$$

where  $\sigma'_{\text{PSII}}$  ( $\text{q } \text{\AA}^{-2}$ ) is the functional absorption cross-section at the ambient irradiance,  $f'$  is the

proportion of functional reaction centres at the ambient irradiance,  $\phi_{\text{RC}}$  is the quantum yield of photochemistry within PSII (default  $1 \text{ e}^- \text{ q}^{-1}$ ), and  $6.022 \times 10^{-3}$  is a conversion factor to a molar ratio and per square meter.

The irradiance-dependence of  $P_b$  and the  $P_f$  was determined using the least-squares fitting procedure on the model of Webb *et al.* (1974), as no apparent photoinhibition was observed.

$$P_i = P_{\text{max}} \left[ 1 - e^{(-\alpha E_{d(i)}/P_{\text{max}})} \right] \quad (3)$$

where  $P_i$  and  $E_{d(i)}$  refer to either  $P_f$  and  $E_d(\text{FRR})$  in the case of the FRR measurements, or to  $P_b$  and  $E_d$  in the case of the  $^{14}\text{C}$  measurements.  $\alpha$  is the initial slope of the resulting  $P$ - $E$  curve [ $^{14}\text{C}$ -based:  $\text{mol C} (\text{mol chl } a)^{-1} \text{ s}^{-1} (\mu\text{mol quanta } \text{m}^{-2} \text{ s}^{-1})^{-1}$ , FRR-based:  $\text{mol e}^- (\text{mol RC})^{-1} \text{ s}^{-1} (\mu\text{mol quanta } \text{m}^{-2} \text{ s}^{-1})^{-1}$ ], and  $P_{\text{max}}$  is a theoretical maximum productivity ( $^{14}\text{C}$ -based:  $\text{mol C} (\text{mol chl } a)^{-1} \text{ s}^{-1}$ , FRR-based:  $\text{mol e}^- (\text{mol RC})^{-1} \text{ s}^{-1}$ ).

### Statistics

The Kruskal-Wallis ANOVA detected the depth-dependent differences in variable fluorescence parameters  $q_p$ ,  $\Delta F/F'_m$ , and  $\sigma'_{\text{PSII}}$ . If any statistical differences occurred, pairwise *a posteriori* comparisons were probed with Mann-Whitney's  $U$ -test. A non-linear regression analysis clarified the dependence between  $P_f$  and  $P_b$ .

## Results

### Radiometric measurements

The changes in cloudiness, and the sea swell introduced deviations from the typical exponential waning of light with depth (Fig. 2). This had a direct influence on  $P_f$ , and further on the comparison between  $P_f$  and  $P_b$ , as these short-term changes in the *in situ* light environment are usually damped during the hour-scale  $^{14}\text{C}$  incubation periods. This was the case also in this study; the variability in the ratios of the average  $E_d(\text{FRR})$  at 3, 6, and 10 m to that at 1 m, described by the coefficient of variation, was clearly higher (41%, 36% and 43%) than the corresponding values for

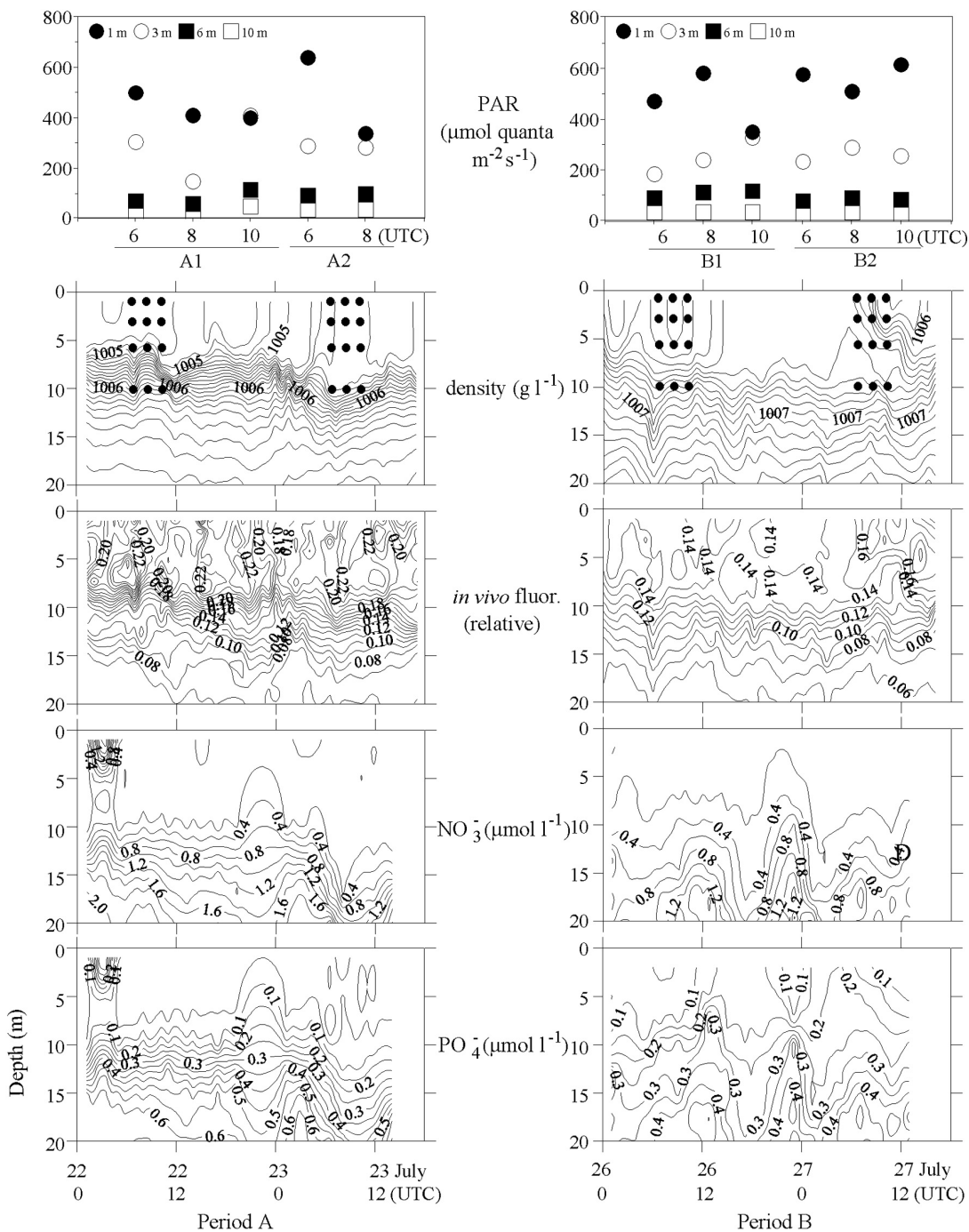


**Fig. 2.** Topmost figures:  $E_0$ (FRR) at each sampling depth. Casts were carried out at 6:00, 8:00, and 10:00 (UTC) on days A1, A2, B1, and B2. Below: density, *in vivo* fluorescence, as well as  $\text{NO}_3^-$  and  $\text{PO}_4^{3-}$  concentrations in the upper 20 m during the study. Left: period A, right: period B. The black dots in the density contours refer to the sampling locations for the  $^{14}\text{C}$  incubations and the FRR measurements.

$E_d$  (5.2%, 5.0% and 10%). Thus, the light field for the FRR measurements was considerably more fluctuating than the one averaged over the  $^{14}\text{C}$  incubation period.

### Physical and chemical milieu

During period A, the main density gradient co-existed with nutricline between 5 and 13 m (Fig. 2). In the surface mixed layer (SML) both the  $\text{NO}_3^-$  and the  $\text{PO}_4^{3-}$  levels were either below the limit of detection ( $0.05 \mu\text{mol l}^{-1}$  for both  $\text{NO}_3^-$  and  $\text{PO}_4^{3-}$ ), or very low, whereas just below the density gradient the concentrations were substantial. Before period B, an upwelling raised markedly  $\text{PO}_4^{3-}$  concentrations in the SML. Due to the intrusion, the density gradient weakened, and the steepest region existed between 8 and 12 m. The *in vivo* fluorescence levels decreased in the SML, as compared with A, whereas the density increased there mainly due to decreased temperature (data not shown).

### Biological environment

Cyanophytes, mainly *Aphanizomenon flos-aquae* (Cyanophyceae), dominated the phytoplankton community in the SML; this group contained >50% of the algal biomass (ww). Dinoflagellates, in turn, dominated the algal community below the main density gradient (~40% of the biomass), with *Heterocapsa rotundata* as the dominant species. The level of chl *a* varied only moderately in the surface layer; from 2.5 to 3.8, and from 1.1 to  $2.7 \mu\text{g l}^{-1}$  during periods A and B, respectively. However, the level of chl *a* at 10 m was only 69% of the average of the values at 1, 3, and 6 m. The  $^{14}\text{C}$ -based biomass-specific *in situ* PP ( $P_b$ ) varied from 0.0110 to  $0.163 \text{ mol C (mol chl } a)^{-1} \text{ s}^{-1}$  (Table 1). The  $P_b$  values at 3, 6, and 10 m were on average 90%, 49% and 15% of that at 1 m, respectively.

The coefficient of variation for  $P_b$  observations at 1 m during the study was only 6.7% suggesting that temporal variability was not likely to explain any differences between  $P_f$  and  $P_b$ . The apparent temporal stability in biological parameters was probably due to the rather stable

upper part of the water column during the study, even though a warmer water mass in the upper 5 m entered into the study area on day B2 (Fig. 2). Hence, the scope of discussion was directed to the vertical variability of the variable fluorescence and photosynthetic parameters.

### Variable fluorescence parameters

During the study the functional ( $\Delta F/F'_m$ ) and the maximum ( $F_v/F_m$ ) photosynthetic energy conversion efficiencies varied between 0.29 and 0.50, and between 0.31 and 0.51, respectively (Table 1). Both  $F_v/F_m$  and  $\Delta F/F'_m$  had their maxima at 6 m;  $\Delta F/F'_m$  was significantly greater at that depth than at any other ( $p < 0.05$ ), while  $F_v/F_m$  at that depth was significantly greater than at 3 and 10 m ( $p < 0.05$ ). The ratio of  $\Delta F/F'_m$  to  $F_v/F_m$  was, on average, 0.89, 0.93, 0.97, and 0.99 at 1, 3, 6, and 10 m, respectively; their difference was significant in the upper 6 m ( $p < 0.05$ , pairwise *t*-test on depths,  $n = 11$ ). The photochemical quenching ( $q_p$ ) increased steadily with depth (Table 1). The depthwise differences, however, were not statistically significant. The range of  $q_p$  was from 0.57 to 0.91, suggesting that the resident phytoplankton community was only moderately photoinhibited during the study. The functional absorption cross-section of PSII at ambient irradiance ( $\sigma_{\text{PSII}}$ ) varied between 290 and  $420 \text{ \AA}^2 \text{ q}^{-1}$  (Table 1). It expressed decreased levels at 1 and 10 m, and the difference between 6 and 10 m was significant ( $p < 0.05$ ). The fluorescence-based *in situ* photosynthetic electron flow ( $P_f$ ) varied from 13.5 to  $471 \text{ mol e}^- (\text{mol RC})^{-1} \text{ s}^{-1}$  (Table 1). The  $P_f$  values at 3, 6, and 10 m were on average 85%, 38% and 12% of that at 1 m, respectively.

### The relation between the variable fluorescence-based and the $^{14}\text{C}$ -based PP

The dependence between  $P_b$  and  $P_f$  was not linear (Fig. 3). The deviation from a linear relation between the parameters started to appear at irradiance levels above  $200 \mu\text{mol quanta m}^{-2} \text{ s}^{-1}$ . Below this level the ratio of  $P_f$  to  $P_b$  was rather constant. As suggested by the light-saturation

**Table 1.** Parameters measured by the FRR fluorometer ( $E_d(\text{FRR})$ ,  $\sigma_{\text{PSII}}$ ,  $\Delta F/F'_m$ ,  $q_p$ , and  $P_t$ ), and parameters related to the  $^{14}\text{C}$  incubations ( $E_d$  and  $P_b$ ) tabulated by single sampling depth on a study day, by day (all depths), and during the entire study. For parameters and units, see Appendix. Averages  $\pm$  standard deviations are given. Observed ranges (minimum–maximum) are given in parentheses if the number of observations is 2. Number of observations: at a single sampling depth: (A1, B1, B2) = 3, A2 = 2. Otherwise: \* = 12; \*\* = 8; \*\*\* = 44.

Depth	$E_d(\text{FRR})$	$\sigma_{\text{PSII}}$	$\Delta F/F'_m$	$q_p$	$P_t$	$E_d$	$P_b$
A1							
1	436 $\pm$ 56	345 $\pm$ 46	0.383 $\pm$ 0.064	0.724 $\pm$ 0.042	378 $\pm$ 35	360 $\pm$ 100	0.139 $\pm$ 0.0099
3	289 $\pm$ 130	349 $\pm$ 18	0.418 $\pm$ 0.061	0.724 $\pm$ 0.064	266 $\pm$ 79	153 $\pm$ 38	0.129 $\pm$ 0.010
6	82.2 $\pm$ 29	390 $\pm$ 35	0.479 $\pm$ 0.022	0.788 $\pm$ 0.016	109 $\pm$ 22	51.8 $\pm$ 13	0.0487 $\pm$ 0.012
10	25.1 $\pm$ 18	321 $\pm$ 21	0.403 $\pm$ 0.006	0.849 $\pm$ 0.016	25.2 $\pm$ 18	13.4 $\pm$ 3.4	0.0159 $\pm$ 0.0045
All depths*	208 $\pm$ 180	351 $\pm$ 38	0.421 $\pm$ 0.054	0.771 $\pm$ 0.064	195 $\pm$ 150	144 $\pm$ 150	0.0832 $\pm$ 0.055
A2							
1	490 (340–640)	313 (303–323)	0.350 (0.33–0.37)	0.788 (0.78–0.79)	383 (300–470)	567 (510–620)	0.123 (0.12–0.13)
3	283 (280–285)	330 (329–332)	0.414 (0.41–0.42)	0.792 (0.79–0.80)	284 (270–300)	230 (210–250)	0.0999 (0.099–0.100)
6	94.6 (92–97)	319 (303–334)	0.496 (0.49–0.50)	0.902 (0.88–0.93)	125 (120–130)	81.3 (75–87)	0.0489 (0.042–0.056)
10	35.5 (35–36)	345 (342–347)	0.477 (0.47–0.48)	0.836 (0.83–0.84)	45.1 (44–46)	21.7 (21–23)	0.0159 (0.015–0.016)
All depths**	226 $\pm$ 210	327 $\pm$ 16	0.434 $\pm$ 0.062	0.829 $\pm$ 0.051	209 $\pm$ 150	225 $\pm$ 230	0.0720 $\pm$ 0.045
B1							
1	468 $\pm$ 120	336 $\pm$ 15	0.250 $\pm$ 0.004	0.849 $\pm$ 0.073	307 $\pm$ 73	594 $\pm$ 28	0.124 $\pm$ 0.029
3	250 $\pm$ 74	350 $\pm$ 34	0.333 $\pm$ 0.043	0.884 $\pm$ 0.020	232 $\pm$ 42	261 $\pm$ 16	0.107 $\pm$ 0.021
6	107 $\pm$ 16	348 $\pm$ 17	0.431 $\pm$ 0.027	0.919 $\pm$ 0.020	135 $\pm$ 17	86.5 $\pm$ 5.8	0.0664 $\pm$ 0.032
10	34.9 $\pm$ 1.0	316 $\pm$ 20	0.398 $\pm$ 0.023	0.920 $\pm$ 0.051	37.4 $\pm$ 2.3	25.6 $\pm$ 2.1	0.0235 $\pm$ 0.011
All depths*	215 $\pm$ 180	338 $\pm$ 24	0.353 $\pm$ 0.076	0.893 $\pm$ 0.050	178 $\pm$ 110	242 $\pm$ 230	0.0803 $\pm$ 0.046
B2							
1	568 $\pm$ 51	355 $\pm$ 37	0.238 $\pm$ 0.051	0.555 $\pm$ 0.030	248 $\pm$ 71	631 $\pm$ 52	0.113 $\pm$ 0.010
3	259 $\pm$ 26	336 $\pm$ 19	0.433 $\pm$ 0.024	0.763 $\pm$ 0.042	268 $\pm$ 52	254 $\pm$ 17	0.108 $\pm$ 0.018
6	86.6 $\pm$ 5.3	337 $\pm$ 8.4	0.473 $\pm$ 0.012	0.798 $\pm$ 0.036	102 $\pm$ 6.5	92.6 $\pm$ 6.4	0.0655 $\pm$ 0.0097
10	32.7 $\pm$ 5.7	327 $\pm$ 13	0.430 $\pm$ 0.048	0.821 $\pm$ 0.047	35.6 $\pm$ 12	28.6 $\pm$ 1.9	0.0183 $\pm$ 0.0029
All depths*	237 $\pm$ 220	339 $\pm$ 22	0.393 $\pm$ 0.100	0.734 $\pm$ 0.120	163 $\pm$ 110	251 $\pm$ 250	0.0762 $\pm$ 0.041
The entire study***							
1	490 $\pm$ 110	339 $\pm$ 31	0.301 $\pm$ 0.076	0.724 $\pm$ 0.125	324 $\pm$ 85	535 $\pm$ 130	0.125 $\pm$ 0.019
3	269 $\pm$ 71	342 $\pm$ 21	0.398 $\pm$ 0.055	0.791 $\pm$ 0.074	261 $\pm$ 50	224 $\pm$ 52	0.112 $\pm$ 0.018
6	92.3 $\pm$ 18	351 $\pm$ 33	0.467 $\pm$ 0.030	0.847 $\pm$ 0.067	117 $\pm$ 19	77.7 $\pm$ 19	0.0588 $\pm$ 0.020
10	31.7 $\pm$ 9.6	326 $\pm$ 18	0.422 $\pm$ 0.038	0.859 $\pm$ 0.052	35.0 $\pm$ 12	22.4 $\pm$ 6.6	0.0191 $\pm$ 0.0069

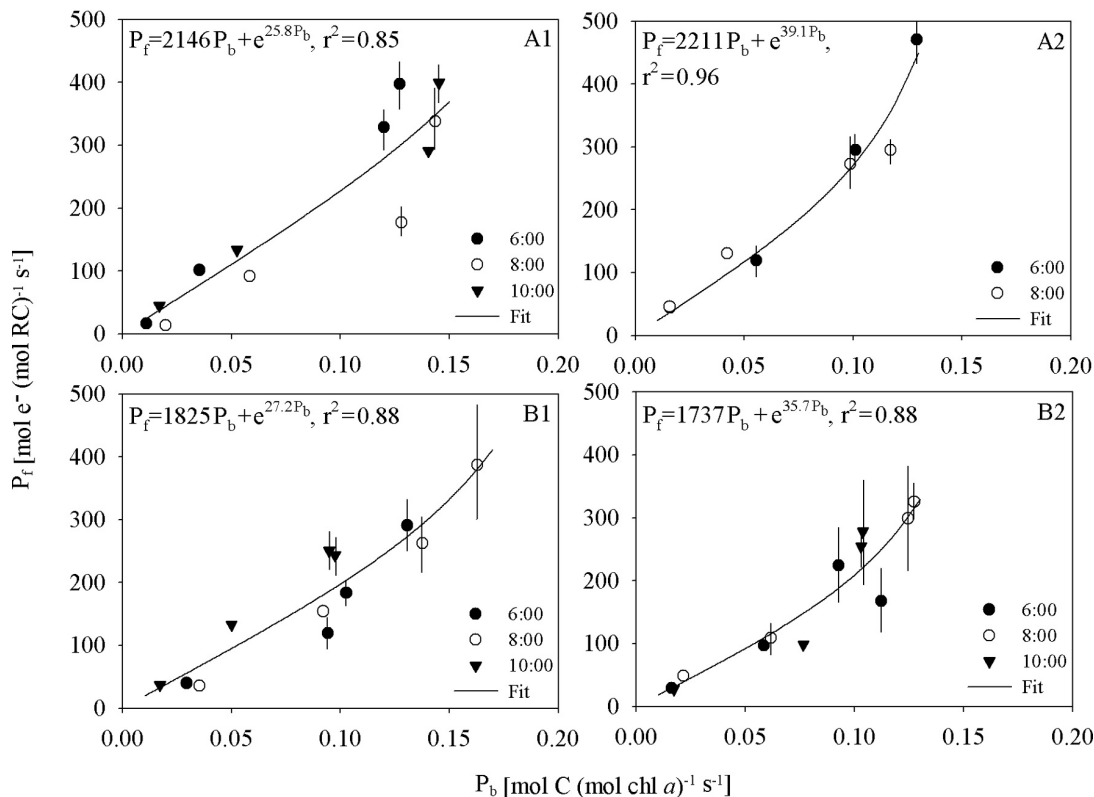


**Fig. 3.** The relation between  $P_f$  and  $P_b$  during days A1, A2, B1, and B2. For parameters and units, see Appendix. The resulting fit of a non-linear regression  $P_f = xP_b + e^{(yP_b)}$  is shown as a solid line, and the standard deviations of  $P_f$ , determined from the three middlemost replicates of a total of five, are shown as vertical solid lines. Lines shorter than the size of the symbols are not shown.  $r^2$  = coefficient of determination.

parameter  $E_k$ , this discrepancy was caused by  $P_b$  reaching its saturation ( $P_{max}$ ) at lower levels of incident irradiance than  $P_f$  did (Fig. 4).  $E_k$ , defined as  $P_{max}/\alpha$ , represents the optimal irradiance level for photosynthesis. Actually,  $P_f$  clearly reached  $P_{max}$  only on day B2.

The coefficients of determination ( $r^2$ ) in non-linear models between  $P_f$  and  $P_b$  were fairly good ( $> 0.85$  for any study day, Fig. 3), but this can be expected, as both of them are largely governed by the exponential vertical pattern of irradiance. The parameters determined by the FRR fluorometer —  $\sigma_{PSII}$ ,  $\Delta F/F'_m$ , and  $q_p$  — actually prevent  $P_f$  from being determined solely by irradiance. Therefore, the productivities were divided by irradiance to obtain information about the light utilization efficiency (LUE) of the resident phytoplankton community. The <sup>14</sup>C-based LUE decreased much more rapidly, as compared with the FRR-based one (Fig. 5), thus corroborating

the result obtained with the  $P$ - $E$  curves. The difference is substantial; the <sup>14</sup>C-based LUE was decreased to near-zero level while the FRR-based LUE was still half of its maximum.

## Discussion

### The dependence between the two techniques under comparison

Whenever novel techniques are compared with widely-used ones, the usual key questions to be answered are how well the new technique reproduces the variability obtained by the widely-used one, and which characteristics of the new technique are responsible for the observed discrepancies. This study cannot be regarded as a mere validation of the FRR technique against the <sup>14</sup>C technique, because the latter technique

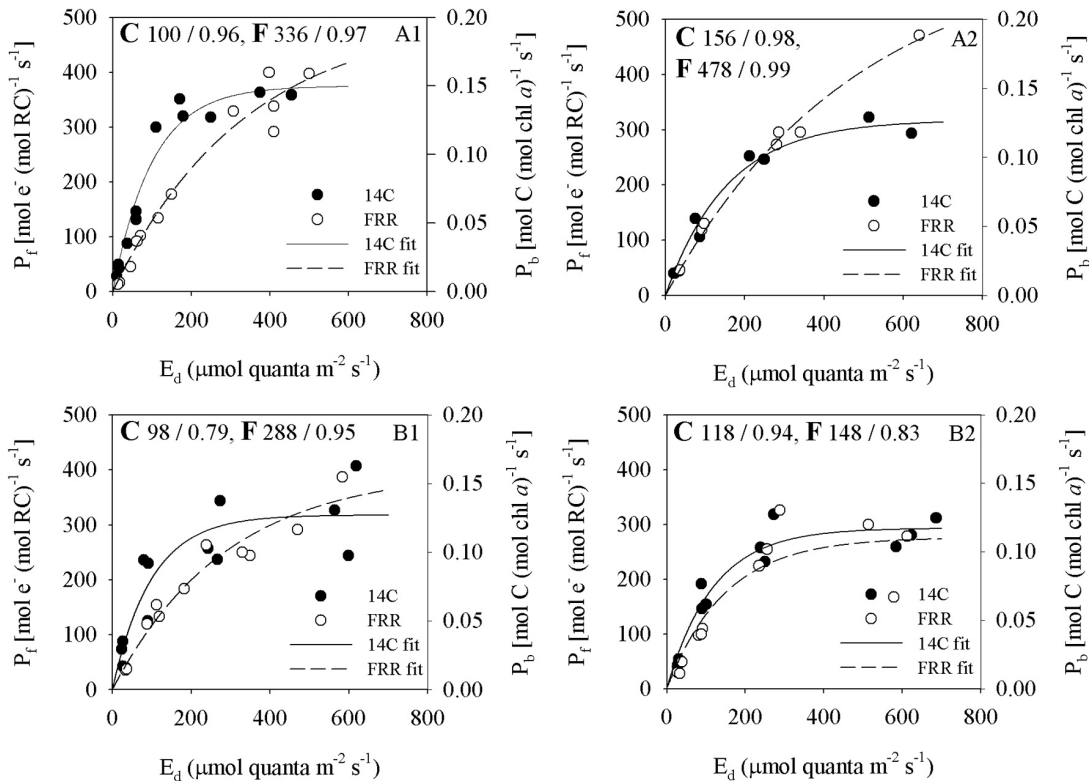


**Fig. 4.** The irradiance-dependence of  $P_f$  and  $P_b$  during days A1, A2, B1, and B2. For parameters and units, see appendix. The resulting fits are expressed as solid ( $^{14}\text{C}$ ), and dashed (FRR) lines. Note: differing from the general nomenclature in this paper,  $E_d$  refers both to  $E_d(\text{FRR})$  and  $E_d$ . The resulting fits are expressed as  $E_k/r^2$  values, the letters preceding are C =  $^{14}\text{C}$ , F = FRR.  $E_k$  is the light-saturation parameter ( $\mu\text{mol quanta m}^{-2} \text{s}^{-1}$ ), and  $r^2$  is the coefficient of determination describing the goodness of fit for Eq. 3.

itself does by no means represent the absolute measurement standard in the primary production field (Bender *et al.* 1987, Grande *et al.* 1989). The latter question, therefore, concerns both the techniques under comparison. However, as the shortcomings of the  $^{14}\text{C}$  technique are well known — e.g. the problems with sampling and incubation (Marra 2002) — and because of the universality of the  $^{14}\text{C}$  technique, I will consider  $^{14}\text{C}$ -based estimates as “true” values, and will concentrate on the mechanisms affecting the photosynthetic electron flow as possible reasons for the observed discrepancy.

The non-linearity between the FRR-based and the  $^{14}\text{C}$ -based PP observed here represents a new evidence for a non-linear relation between the photosynthetic electron flow and the fixation of C (e.g. Boyd *et al.* 1997, Hartig *et al.* 1998, Barranguet and Kronkamp 2000). These studies were not carried out using the FRR technique,

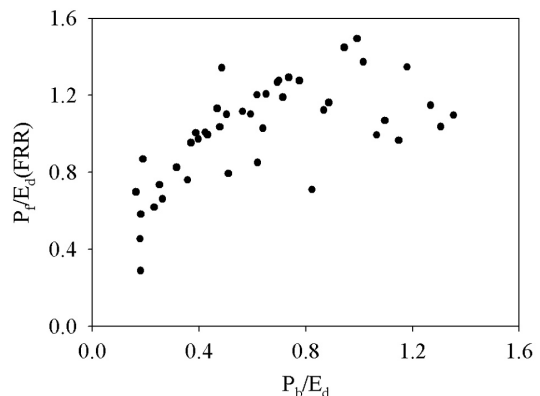


**Fig. 5.** The light utilization efficiency of phytoplankton community approached by the  $^{14}\text{C}$  and the FRR techniques. The dataset represents the whole study. Y-axis: the FRR-based efficiency ( $P_f/E_d(\text{FRR})$ ), x-axis: the  $^{14}\text{C}$ -based efficiency ( $P_b/E_d$ ).

though. Comparisons made between the  $^{14}\text{C}$  and the FRR technique are so far scarce (Babin *et*

al. 1996, Suggett *et al.* 2001), but also suggest that this relation is not straightforward. The FRR technique measures the rate of electron flow through PSII in the electron transport chain (ETC) in the light reactions of the photosynthetic machinery (Falkowski and Kolber 1995). The function of PSII — the charge separation — and the fixation of C are located quite far from each other in the cascade of photosynthetic processes, and are not as closely coupled as the charge separation and oxygen formation (Serôdio 2003). Hence, the observed non-linearity between  $P_f$  and  $P_b$  at high irradiance levels can be related to various factors that are influencing either on the rate of electron transport in the ETC, or on the fate of electrons after the ETC.

The two mechanisms taking place in the ETC — the cyclic electron flows around PSII and photosystem I (PSI) — circulate electrons in the ETC, and thus, lower the rate of the linear electron flow to the terminal electron acceptors of the ETC, especially NADPH. This leads to the lowered rate of C fixation. Neither of these mechanisms decreases the electron flow through PSII that is measured by the FRR technique, however. In the cyclic electron flow around PSII, the electrons are returned from the acceptor side of PSII to its donor side, leading to a deviation from a linear relation between the  $O_2$  flash yield and the variable fluorescence yield (Falkowski *et al.* 1986, Prasil *et al.* 1996). This process is engaged at saturating irradiance levels, i.e., when the plastoquinone pool is reduced (Lavaud *et al.* 2002), suggesting that this mechanism has a photoprotective role. The cyclic electron flow around PSI returns the electrons from ferredoxin, which acts as one of the reductants produced by the ETC, back to the donor side of PSI (Falkowski and Raven 1997). This mechanism is an important source of ATP, especially to N-fixing cyanobacteria, and has a function in the regulation of photosynthesis (Falkowski and Raven 1997).

The photosynthetic light reactions are coupled with fixation of C by the generated NADPH (Falkowski and Raven 1997). However, electron sinks other than  $CO_2$  cause discrepancy between the fixation of C and the photosynthetic electron flow at irradiance levels  $> E_k$  where photosynthesis is limited by the utilization of NADPH, not by its production (Sakshaug *et al.* 1997). These

processes include the Mehler reaction and photorespiration. In the Mehler reaction, an electron donated by ferredoxin on the acceptor side of PSI reduces an evolved  $O_2$  molecule, not the usual terminal electron acceptor  $NADP^+$ . This process leads to the formation of a superoxide radical, eventually leading to the formation of an  $H_2O$  molecule. Hence, this process is called the water–water cycle (Heber 2002). In this process there is no net  $O_2$  or electron gain. The Mehler reaction has been observed in both cyanophytes and chlorophytes, and it is not considered to be important at irradiances  $< E_k$  (Kana 1992, Rees *et al.* 1992). The proportion of electrons re-channeled by the Mehler reaction can be 10%–50% of the total linear electron transport (Furbank *et al.* 1992, Kana 1993). The oxygenase activity of the carboxylating enzyme (ribulose bis-phosphate carboxylase/oxygenase, RuBisCO) called photorespiration, can also affect the relation between  $P_f$  and  $P_b$  by decreasing the rate of C fixation. This process is stimulated by high *in vivo* ratios of  $O_2$  to  $CO_2$  (Masojídek *et al.* 2001). However, photorespiration is not considered to be quantitatively important in most representatives of phytoplankton, because photorespiratory activity is reduced by the  $CO_2$  concentrating mechanisms (Ogren 1984, Flameling and Kronkamp 1998).

Dark respiration, which lowers the  $^{14}C$  estimate to an unknown extent, is observed to vary from below 1% to up to 50% of the gross photosynthesis (Geider and Osborne 1989, and references therein). Respiratory processes are thought to represent a constant fraction of the growth rate (Geider 1992, Falkowski and Raven 1997). Thus, they should not be responsible for the apparent non-linearity between  $P_f$  and  $P_b$ . Nevertheless, in their comparison between the electron-flow-based and the  $O_2$ -based PP techniques, Flameling and Kronkamp (1998) suggested that mitochondrial respiration rates are controlled by light intensity, thus participating in the observed non-linearity between the fixation of C and the photosynthetic electron flow.

### Deviations from the general dependence

Given the rather small number of replicates, the deviations from the regression fits were fairly

moderate (Fig. 3), and mainly caused by the methodology. The measurement period for  $P_f$  is two to three orders of magnitude shorter than for  $P_b$ .  $P_f$  is thus subject to the momentary incident illumination at the time of measurement, whereas  $P_b$  is largely determined by the average irradiance level over the incubation period. This methodological discrepancy is reflected in the shape of the vertical irradiance profiles, as the underwater light milieu is far from stable in any temporal scale. The FRR technique is sensitive to the short-term variability in the underwater light field caused mainly by variations in cloudiness as well as by the wave-induced vertical movement of the instruments attached to the vessel. The closer to the surface the measurements are carried out, the more pronounced this variability will be. Day B1, with a relatively low  $r^2$  value for the light-dependence of the  $^{14}\text{C}$  technique (Fig. 4), did not differ notably from the three others regarding average wind velocity (data not shown), but the degree of cloudiness on that day did vary markedly. Taken together, marked temporal changes in *in situ* irradiance during the FRR measurements represent a substantial source of error for the FRR-based estimates of PP. Consequently, the FRR measurements during rough seas should be avoided.

### The vertical variability of the algal photosynthetic efficiency

The photosynthetic efficiency of phytoplankton in the measured part of the water column, as estimated by  $\Delta F/F'_m$ , could be divided into three layers: reduced levels in the near-surface layer due to inhibiting effect of supraoptimal irradiance, the layer beneath this having the highest levels, and the deepest layer measured inhabited by a senescent algal population characterized by lowered levels (Table 1). A similar three-part pattern has also been observed in truly oceanic environments (Babin *et al.* 1996, M. Raateoja *et al.* unpubl. data).

The depth of the SML was rather typical for the late-summer situation in the Baltic Sea — rather shallow — during the study, and the algal community inhabiting the layer were subject to rather high average irradiance levels. However,

inhibition of the photosynthetic potential of the algae by excess light was not observed through the whole SML;  $q_p$  and  $\Delta F/F'_m$  — describing the fraction of reaction centres (RC) capable of participating in photosynthetic process, and the activity of those RCs, respectively — decreased towards the surface only in the upper 6 m (Table 1). As the photoadaptive responses of the algal cells depend on the time scales for vertical mixing and the photoacclimation rate (Cullen and Lewis 1988), the mixing rates caused by the fairly strong wind (from 7 to 10 m s<sup>-1</sup> during the study, data not shown) were apparently not high enough to prevent the algae spending too long time at supra-optimal irradiance levels near to the surface.

Whereas the inorganic nutrient levels were at the limit of detection or very low in the SML, the algal community in and below the main density gradient was associated with nutrient levels that probably were not limiting photosynthesis (Fig. 2). Bearing in mind the enhancement of the photosynthetic performance due to the higher nutrient availability (e.g. Cleveland and Perry 1987, Kolber *et al.* 1988, Herzig and Falkowski 1989, Geider *et al.* 1993), and the tendency for phytoplankton cells to increase their light utilization efficiency with depth, i.e., towards lower irradiance levels, the decrease in  $\Delta F/F'_m$  from 6 m downwards was unexpected. This decrease was probably characteristic of the senescent algal population which had descended into the density gradient. An aspect not to be forgotten is the possible influence of the changing taxonomic composition of the resident phytoplankton community between the SML and the main density gradient. The taxonomic effects on  $\Delta F/F'_m$  need, however, further study.

### Concluding remarks

The future vision of the use of the FRR technique as a reliable tool measuring PP is primarily obscured by its non-linear relation with the  $^{14}\text{C}$  technique. This non-linearity itself is not so much of an obstacle because the  $^{14}\text{C}$  technique is not an unambiguous measuring tool either. Rather, it is problematic because it complicates the validation of the FRR outcome with the  $^{14}\text{C}$  one, which is an essential step in the develop-

ment of the FRR technique for remote sensing purposes. The not so close coupling between the two processes studied here — the function of PSII and the fixation of C — justifies a doubt, if the rate of photosynthetic electron flow may never be used as a substituting/complementing tool for the fixation of C. Anyway, further study is required before the impact of the various physiological mechanisms acting as electron sinks can be identified and quantified. Only after this can the FRR-based PP estimates be reliably interpreted for remote sensing purposes. If feasible for the remote sensing of aquatic systems, the FRR technique will be a valuable tool that acquires high-frequency information about the PP over large oceanic systems.

The PP is largely governed by the irradiance, except in the very near-surface layer. The impact of the irradiance on the comparison in this paper was emphasized by the fact that this study was restricted to a rather narrow chl *a* range. Hence, these results represent the late summer algal community, and should be used with caution for seasonal algal bloom periods characterized by high variability in chl *a* levels.

The estimates of the PP by the two techniques were based on periods of time of extremely unequal length. This factor introduced discrepancy into the comparison between the techniques, but also stressed the advantages of the dynamic nature of the FRR technique. This is of especial value in the Baltic Sea, where hydrography operates on rather small scales, as compared with the world's oceans. The problems concerning the estimation of the PP with the FRR technique do not reduce in any way the value of the FRR-based photosynthetic parameters describing the photosynthetic efficiency, and the light-adaptive state of phytoplankton.

*Acknowledgements:* I thank the Finnish Institute of Marine Research for offering the laboratory facilities on-board R/V "Aranda", and for the time of its personnel to provide the CTD, nutrient, and chl *a* data; J. Seppälä and H. Kuosa for their revealing comments; M. Huttunen for providing the taxonomic data; R. Olsonen and K. Kahma for their statistical expertise; R. King for improving the language; and anonymous reviewers for improving the article itself. This study was funded by MITEC, Contract MAS3-CT97-0114, in the European Commission MAST Program, Maj and Tor Nessling Foundation, Onni Talas foundation, and the Finnish Institute of Marine Research.

## References

- Babin M., Morel A., Claustre H., Bricaud A., Kolber Z. & Falkowski P.G. 1996. Nitrogen- and irradiance-dependent variations of the maximum quantum yield of carbon fixation in eutrophic, mesotrophic and oligotrophic marine systems. *Deep-Sea Res.* 43: 1241–1272.
- Baltic Marine Environment Protection Commission 1988. Guidelines for the Baltic Monitoring Programme for the third stage. Part D. Biological determinants. *Baltic Sea Environ. Proc.* No. 27D.
- Barranguet C. & Kronkamp J. 2000. Estimating primary production rates from photosynthetic electron transport in estuarine microphytobenthos. *Mar. Ecol. Prog. Ser.* 204: 39–52.
- Behrenfeld M.J., Prasil O., Kolber Z.S., Babin M. & Falkowski P.G. 1998. Compensatory changes in photosystem II turnover rates protect photosynthesis from photoinhibition. *Photosyn. Res.* 58: 259–268.
- Bender M., Grande K., Johnson K., Marra J., Williams P.L.B., Sieburth J., Pilson M., Langdon C., Hitchcock G., Orchardo J., Hunt C., Donaghay P. & Heinemann K. 1987. A comparison of four methods for determining planktonic community production. *Limnol. Oceanogr.* 32: 1085–1098.
- Boyd P.W., Aiken J. & Kolber Z. 1997. Comparison of radiocarbon and fluorescence based (pump and probe) measurements of phytoplankton photosynthetic characteristics in the Northeast Atlantic Ocean. *Mar. Ecol. Prog. Ser.* 149: 215–226.
- Buch K. 1945. Kolsyrejämvikten i Baltiska havet. *Fennia* 68: 1–208.
- Chekyaluk A.M., Hoge F.E., Wright S.W. & Swift R.N. 2000. Short-pulse pump-and-probe technique for airborne laser assessment of photosystem II photochemical characteristics. *Photosyn. Res.* 66: 33–44.
- Cleveland J.S. & Perry M.J. 1987. Quantum yield, relative specific absorption and fluorescence in nitrogen-limited *Chaetoceros cracilis*. *Mar. Biol.* 94: 489–497.
- Cullen J.J. & Lewis M.R. 1988. The kinetics of algal photoadaptation in the context of vertical mixing. *J. Plank. Res.* 10: 1039–1063.
- Falkowski P.G. 1992. Molecular ecology of phytoplankton photosynthesis. In: Falkowski P.G. & Woodhead A.D. (eds.), *Primary productivity and biogeochemical cycles in the sea*, Plenum, New York, pp. 47–67.
- Falkowski P.G., Fujita Y., Ley A. & Mauzerall D. 1986. Evidence for cyclic electron flow around photosystem II in *Chlorella pyrenoidosa*. *Plant Physiol.* 81: 310–312.
- Falkowski P.G. & Kolber Z. 1993. Estimation of phytoplankton photosynthesis by active fluorescence. *ICES Mar. Sci. Symp.* 197: 92–103.
- Falkowski P.G. & Kolber Z. 1995. Variations in chlorophyll yields in phytoplankton in the world oceans. *Aust. J. Plant Physiol.* 22: 341–355.
- Falkowski P.G. & Raven J.A. 1997. *Aquatic photosynthesis*, Blackwell Science.
- Falkowski P., Wyman K., Ley A.C. & Mauzerall D. 1986. Relationship of steady-state photosynthesis to fluorescence in eucaryotic algae. *Biochim. Biophys. Acta* 849:

- 183–192.
- Flameling I.A. & Kronkamp J. 1998. Light dependence of quantum yields for PSII charge separation and oxygen evolution in eucaryotic algae. *Limnol. Oceanogr.* 43: 284–297.
- Furbank R.T., Badger R.M. & Osmond C.B. 1992. Photosynthetic oxygen exchange in isolated cells and chloroplasts of C3 plants. *Plant Physiol.* 70: 927–931.
- Gargas E. 1975. A manual for phytoplankton production studies in the Baltic. *BMB Publ.* 2: 1–88.
- Geider R.J. 1992. Respiration: taxation without representation? In: Falkowski P.G. & Woodhead A.D. (eds.), *Primary productivity and biogeochemical cycles in the sea*, Plenum, New York, pp. 333–360.
- Geider R.J., La Roche J., Greene R.M. & Olairola M. 1993. Response of the photosynthetic apparatus of *Phaeodactylum tricornutum* (bacillariophyceae) to nitrate, phosphate, or iron limitation. *J. Phycol.* 29: 755–766.
- Geider R.J. & Osborne B.A. 1989. Respiration and microalgal growth: a review of the quantitative relationship between dark respiration and growth. *New Phytol.* 112: 327–341.
- Grande K.D., Williams P.J.LeB., Marra J., Purdie D.A., Heinemann K., Eppley R.W. & Bender M. 1989. Primary production in the North Pacific gyre: a comparison of rates determined by the <sup>14</sup>C, O<sub>2</sub> concentration and <sup>18</sup>O methods. *Deep-Sea Res.* 36: 1621–1634.
- Grasshoff K., Kremling K. & Ehrhardt M. (eds.) 1999. *Methods of seawater analysis*, 3rd ed., Wiley-VCH.
- Hartig P., Wolfstein K., Lippemeier S. & Colijn F. 1998. Photosynthetic activity of natural microphytobenthos populations measured by fluorescence (PAM) and <sup>14</sup>C-tracer methods: a comparison. *Mar. Ecol. Prog. Ser.* 166: 53–62.
- Heber U. 2002. Irrungen, wirrungen? The Mehler reaction in relation to cyclic electron transport in C3 plants. *Photosyn. Res.* 73: 223–231.
- Herzig R. & Falkowski P. 1989. Nitrogen limitation in *Isochrysis galbana* (haptophyceae). I. Photosynthetic energy conversion and growth efficiencies. *J. Phycol.* 25: 462–471.
- Hiscock M.R., Marra J., Smith Jr. W.O., Goericke R., Measures C., Vink S., Olson R.J., Sosik H. & Barber R.T. 2003. Primary productivity and its regulation in the Pacific sector of the Southern Ocean. *Deep-Sea Res.* 50: 533–558.
- Kana T.M. 1992. Relationship between photosynthetic oxygen cycling and carbon assimilation in *Synechococcus* WTH7803 (Cyanophyta). *J. Phycol.* 28: 304–308.
- Kana T.M. 1993. Rapid oxygen cycling in *Trichodesmium thiebautii*. *Limnol. Oceanogr.* 38: 18–24.
- Kolber Z.S. & Falkowski P.G. 1992. Fast Repetition Rate (FRR) fluorometer for making *in situ* measurements of primary productivity. In: *Proceedings of Ocean 92 conference*, Newport, Rhode Island, 26–29 September 1992, pp. 637–641.
- Kolber Z.S., Prášil O. & Falkowski P.G. 1998. Measurements of variable fluorescence using fast repetition rate techniques: defining methodology and experimental protocols. *Biochim. Biophys. Acta* 1367: 88–106.
- Kolber Z., Zehr J. & Falkowski P. 1988. Effects of growth irradiance and nitrogen limitation on photosynthetic energy conversion in photosystem II. *Plant Physiol.* 88: 923–929.
- Kononen K., Huttunen M., Hällfors S., Gentien P., Lunven M., Huttula T., Laanemets J., Lilover M., Pavelson J. & Stips A. 2003. Development of a deep chlorophyll maximum of *Heterocapsa triquetra* Ehrenb. at the entrance to the Gulf of Finland. *Limnol. Oceanogr.* 48: 594–607.
- Kononen K., Huttunen M., Kanoshina L., Laanemets J., Moisander P. & Pavelson J. 1999. Spatial and temporal variability of a dinoflagellate-cyanobacterium community under a complex hydrodynamical influence: a case study at the entrance to the Gulf of Finland. *Mar. Ecol. Prog. Ser.* 186: 43–57.
- Krause G.H. & Weis E. 1991. Chlorophyll fluorescence and photosynthesis: the basics. *Annu. Rev. Plant Physiol. Plant Mol. Biol.* 42: 313–349.
- Lavaud J., van Gorkom H.J. & Etienne A.-L. 2002. Photosystem II electron transfer cycle and chlororespiration in planktonic diatoms. *Photosyn. Res.* 74: 51–59.
- Marra J. 2002. Approaches to the measurement of plankton production. In: Williams P.J.LeB., Thomas D.N. & Reynolds C.S. (eds), *Phytoplankton productivity. Carbon assimilation in marine and freshwater ecosystems*, Blackwell Science, pp. 78–108.
- Masojádek J., Grobbelaar J.U., Pechar L. & Koblížek M. 2001. Photosystem II electron transport rates and oxygen production in natural waterblooms of freshwater cyanobacteria during a diel cycle. *J. Plank. Res.* 23: 57–66.
- Moisander P., Rantajarvi E., Huttunen M. & Kononen K. 1997. Phytoplankton community in relation to salinity fronts at the entrance to the Gulf of Finland, Baltic Sea. *Ophelia* 46: 187–203.
- Niemi M., Kuparinen J., Uusi-Rauva A. & Korhonen K. 1983. Preparation of <sup>14</sup>C-labeled algal samples for liquid scintillation counting. *Hydrobiologia* 106: 149–156.
- Ogren W.L. 1984. Photorespiration: Pathways, regulation, and modification. *Annu. Rev. Plant Physiol. Plant Mol. Biol.* 35: 415–442.
- Oxborough K.O. & Baker N.R. 1997. Resolving chlorophyll a fluorescence images of photosynthetic efficiency into photochemical and non-photochemical components — calculation of qP and Fv'/Fm' without measuring Fo'. *Photosyn. Res.* 54: 135–142.
- Prasil O., Kolber Z., Perry J.A. & Falkowski P.G. 1996. Cyclic electron flow around photosystem II *in vivo*. *Photosyn. Res.* 48: 395–410.
- Rees D., Lee C.B., Gilmour D.J. & Horton P. 1992. Mechanisms for controlling balance between light input and utilization in the salt tolerant alga *Dunaliella* C9AA. *Photosyn. Res.* 32: 181–191.
- Sakshaug E., Bricaud A., Dannonneau Y., Falkowski P.G., Kiefer D.A., Legendre L., Morel A., Parslow J. & Takahashi M. 1997. Parameters of photosynthesis: definitions, theory and interpretation of results. *J. Plank. Res.* 19: 1637–1670.
- Seródio J. 2003. A chlorophyll fluorescence index to estimate short-term rates of photosynthesis by intertidal microphytobenthos. *J. Phycol.* 39: 33–46.
- Sosik H.M. & Olson R.J. 2002. Phytoplankton and iron

- limitation of photosynthetic efficiency in the Southern Ocean during late summer. *Deep-Sea Res.* 49: 1195–1216.
- Stemann Nielsen E. 1952. The use of radioactive carbon ( $^{14}\text{C}$ ) for measuring organic production in the sea. *J. Cons. Int. Explor. Mer* 18: 117–140.
- Suggett D., Kraay G., Holligan P., Davey M., Aiken J. & Geider R. 2001. Assessment of photosynthesis in a spring cyanobacterial bloom by use of a fast repetition rate fluorometer. *Limnol. Oceanogr.* 46: 802–810.
- Timmermans K.R., Davey M.S., van der Wagt B., Snoek J., Geider R.J., Veldhuis M.J.W., Gerringa L.J.A. & de Baar H.J.W. 2001. Co-limitation by iron and light of *Chaetoceros brevis*, *C. dicaeta* and *C. calcitrans* (Bacillariophyceae). *Mar. Ecol. Prog. Ser.* 217: 287–297.
- Utermöhl H. 1958. Zur Vervollkommnung der Quantitativen Phytoplankton-Methodik. *Mitt. Internat. Verein. Theor. Angew. Limnol.* 9: 1–38.
- Vassiliev I.R., Prasil O., Wyman K.D., Kolber Z., Hanson A.K.Jr., Prentice J.E. & Falkowski P.G. 1994. Inhibition of PS II photochemistry by PAR and UV radiation in natural phytoplankton communities. *Photosyn. Res.* 42: 51–64.
- Voipio A. (ed.) 1981. *The Baltic Sea*, Elsevier Oceanogr. Ser. 30, Elsevier, Amsterdam.
- Webb W.L., Newton M. & Starr D. 1974. Carbon dioxide exchange of *Alnus rubra*: a mathematical model. *Oecologia* 17: 281–291.

Received 20 May 2003, accepted 21 December 2003

## Appendix

Symbol	Explanation
$F_o, F_m$	Initial and maximal <i>in vivo</i> fluorescence yield (relative) in the dark-adapted state in the absence of non-photochemical quenching ( $q_n = 0$ ). $F_o: q_p = 1$ , $F_m: q_p \rightarrow 0$ (never actually reaches zero).
$F, F_m$	Initial and maximal <i>in vivo</i> fluorescence yield (relative) at the ambient irradiance in the presence of non-photochemical quenching ( $q_n \geq 0$ ). $F: 0 < q_p < 1$ , $F_m: q_p \rightarrow 0$ .
$F'_o$	The <i>in vivo</i> fluorescence yield (relative) at the ambient irradiance, subsequently measured after 1 to 2 s dark adaptation ( $q_p = 1$ and $q_n \geq 0$ ).
$q_p$	The photochemical quenching (dimensionless number between 0 and 1), a measure of the proportion of open PSII reaction centres capable of charge separation. $q_p = (F'_m - F)/(F'_m - F'_o)$ .
$q_n$	The non-photochemical quenching, describing the proportion of excited energy dissipated by thermal decay processes (dimensionless number between 0 and 1).
$F_v/F_m, \Delta F/F'_m$	The maximum and functional photosynthetic energy conversion efficiency (dimensionless number), measured in the dark-adapted state and at the ambient irradiance. $F_v/F_m$ represents the upper limit of the overall photosynthetic efficiency. $F_v = (F_m - F_o)$ , and $\Delta F = (F'_m - F)$ .
$\sigma_{\text{PSII}}, \sigma'_{\text{PSII}}$	The functional absorption cross-section of PSII ( $\text{\AA}^2 \text{q}^{-1}$ ) in the dark-adapted state and at the ambient irradiance, representing the effective target size of a PSII antenna.
$f, f'$	The proportion of functional reaction centres (dimensionless number between 0 and 1) in the dark-adapted state and at the ambient irradiance. $f = (F_v/F_m)/0.65$ , and $f' = (\Delta F/F'_m)/0.65$ .
$\phi_{\text{RC}}$	The quantum yield of photochemistry within PSII [ $\text{mol e}^- (\text{mol q})^{-1}$ ].
$P_f$	The fluorescence-based <i>in situ</i> photosynthetic electron flow [ $\text{mol e}^- (\text{mol RC})^{-1} \text{s}^{-1}$ ].
$P_c$	The $^{14}\text{C}$ -based <i>in situ</i> primary productivity ( $\text{mg C m}^{-3} \text{h}^{-1}$ ).
$P_b$	The $^{14}\text{C}$ -based biomass-specific <i>in situ</i> primary productivity [ $\text{mol C} (\text{mol chl a})^{-1} \text{s}^{-1}$ ].
$E_d(\text{FRR})$	The ambient irradiance measured during the FRR casts (PAR, $\mu\text{mol quanta m}^{-2} \text{s}^{-1}$ ).
$E_d$	The ambient irradiance measured during the $^{14}\text{C}$ incubations (PAR, $\mu\text{mol quanta m}^{-2} \text{s}^{-1}$ ).